J Electroceram (2013) 31:159–167
DOI 10.1007/s10832-013-9837-5

Piezoelectric properties of the high temperature MPB $xPbTiO_3$ - $(1-x)[BiScO_3 + Bi(Ni_{1/2}Ti_{1/2})O_3]$ composition

Troy Y. Ansell · David P. Cann

Received: 30 January 2013 / Accepted: 17 June 2013 / Published online: 29 June 2013

Abstract The ternary perovskite $xPbTiO_3$ - $(1-x)[BiScO_3 + Bi(Ni_{1/2}Ti_{1/2})O_3]$ (PT-BS-BNiT), where $x=0.54$ is the morphotropic phase boundary composition, was studied for high temperature ferroelectric applications. Polycrystalline ceramics were prepared using the standard solid-state methods. The stoichiometric ceramic was found to have room temperature dielectric permittivity and loss values at 1 kHz of 1490 and 0.049 respectively. Piezoelectric properties, of the stoichiometric composition, measured included: $P_r=31.0$ μC/cm^2, $E_c=25.0$ kV/cm, $d_{33}=340$ pC/N, $d_{33}^*=896$ pm/V, and a bipolar electromechanical strain of 0.25 %. From these data, the Curie temperature was $T_C=370$ °C and the depoling temperature was $T_D=325$ °C. Processing ceramics with excess bismuth improved the low field piezoelectric coefficients with a maximum of d33=445 pC/N, while increasing the lead content increased the transition temperatures. The depoling and Curie temperatures of all compositions were measured to be between 275 and 400 °C.

Keywords Piezoelectric · Ferroelectric · Perovskite · Lead · Ternary

1 Introduction

Since the discovery of ferroelectricity in Rochelle salt in 1921 [1], many materials exhibiting ferroelectric behavior have been discovered. The most widely used and studied ferroelectric materials include barium titanate ($BaTiO_3$) and lead zirconium titanate ($xPbTiO_3$-(1-x)$PbZrO_3$) or PZT. The latter, PZT, has been used extensively for several ferroelectric applications including ferroelectric random access memory (FeRAM) [2], as a heat sensor and other pyroelectric applications [3], in piezoelectric sensor applications such as in battery and tire pressure sensors [4], and piezoelectric actuator applications such as piezoelectric microelectromechanical (MEMS) systems [5]. In the field of high temperature piezoelectric transducers, PZT remains the standard material though its operating temperature is limited by depolarization processes that become prevalent at temperatures near 150–200 °C [6–8].

High temperature piezoelectric sensors and actuators are of interest for a variety of different applications ranging from commercial turbine engines to deep-sea drilling and interplanetary probes. The dominance of PZT in piezoelectric applications is due to its excellent properties including large piezoelectric coefficients (d_{33}, d_{31}, and d_{15}), high dielectric constant and low dielectric loss, high polarizability, a relatively high transition temperature, and a large degree of solubility which allows a selection of dopants with PZT to engineer the properties of the final device [9].

The composition at the morphotropic phase boundary or MPB (52PT-48PZ) possesses the largest piezoelectric coefficients and coupling factors [10]. The piezoelectric properties of PZT at the MPB include $d_{33}=233$ pC/N, $d_{31}=-93.5$ pC/N, and $d_{15}=494$ pC/N for the un-doped MPB composition [9]. Mechanical coupling in undoped MPB PZT was measured to be $k_P=0.52$, $k_{33}=0.67$, $k_{31}=0.31$, and $k_{15}=0.69$ [9]. Relatively high dielectric constants and a low dissipation factor of 0.004 were also measured for the MPB PZT composition [9]. Relatively high transition temperature or Curie temperature was also reported for MPB PZT at $T_C=386$ °C [9]. Doping and substitution of PZT causes substantial changes in the macroscopic properties previously listed. Donor doping of PZT, such as a soft PZT like Navy type

T. Y. Ansell (✉) · D. P. Cann
Materials Science, School of Mechanical, Industrial, and Manufacturing Engineering, Oregon State University, Corvallis, OR 97331, USA
e-mail: ansellt@onid.orst.edu

D. P. Cann
e-mail: cann@engr.orst.edu

IV/PZT 5H, leads to higher piezoelectric response, d_{33}=750 pC/N, but lowers the transition temperature to T_C~195 °C as compared to un-doped PZT. Acceptor doping, such as in a hard PZT like Navy type II/PZT 5A, also leads to a higher piezoelectric coefficient of d_{33}=375 pC/N, but again the transition temperature is lowered to T_C=370 °C [9–11]. Despite these impressive properties, the Curie temperature of PZT, in both doped and un-doped form, is too low for many high temperature applications. Especially, the rapid degradation of piezoelectric properties of PZT beyond a temperature of ~200 °C effectively limits the use of PZT at elevated temperatures [12]. Therefore, new materials have been developed with the goal of achieving the same or improved piezoelectric properties of PZT with transition temperatures exceeding 400 °C.

Because transition temperatures of PZT-based compositions do not typically exceed 400 °C, alternative families of high temperature piezoelectric perovskite ceramics based on solid solutions with PT have been developed. Some examples of PT based piezoelectric ceramics include binary solid solutions such as ($xPbTiO_3$-(1-x)$BiScO_3$, PT-BS) [11–20], ($xPbTiO_3$-(1-x)$Bi(M',Ti)O_3$, PT-BM′T) [12, 21–25], where M′=Zn, Mg, or Ni, and ($xPbTiO_3$-(1-x)[$Bi(Mg_{1/2}Ti_{1/2})O_3$-$BiFeO_3$-$BiScO_3$], PT-BMTFS) [26]. The MPB composition of PT-BS at x~0.65 [13–15, 19, 20], exhibited a high Curie temperature (T_C=460 °C), high piezoelectric constants (d_{33}=450 pC/N), and dielectric properties comparable to PZT [15, 19]. Added to these impressive improvements over PZT, the upper operating temperature of PT-BS, otherwise known as the depoling temperature, T_D, was found to be approximately 350 °C [12, 18]. Despite these outstanding properties, the expense of Sc_2O_3 makes it desirable to develop a material with the similar improvements over PZT in piezoelectric properties with the same high transition temperatures, T_C and T_D, as PT-BS while replacing scandium in part or in full with another ferroelectrically active cation. For example, Sebastian et al. developed the PT-BMTFS system replacing Sc_2O_3 with Fe_2O_3 to lower the cost of piezoelectric material [26–28].

In previous work, a number of PT based ternary perovskite piezoelectric systems were developed for high temperature applications including ($xPbTiO_3$-(1-x)[$BiScO_3$ + $Bi(Zn_{1/2}Ti_{1/2})O_3$], PT-BS-BZnT), ($xPbTiO_3$-(1-x)[$BiScO_3$ + $Bi(Mg_{1/2}Ti_{1/2})O_3$], PT-BS-BMgT), and ($xPbTiO_3$-(1-x)[$BiScO_3$ + $Bi(Ni_{1/2}Ti_{1/2})O_3$], PT-BS-BNiT) [29]. The PT-BS-BNiT ternary system showed the most promise in achieving high piezoelectric performance with a high T_C and T_D. The MPB composition at x=0.54 (54PT-23BS-23BNiT), exhibited the highest piezoelectric coefficient of d_{33}=376 pC/N and highest remanent polarization of P_r=29.0 μC/cm^2 [29] respectively. This paper will investigate the piezoelectric properties and depolarization temperature of PT-BS-BNiT ternary ceramics as well as to examine the influence of the Bi^{3+} and Pb^{2+} stoichiometry.

2 Experimental

The focus of this work is on the composition xPT-(1-x)[BS-BNiT] with x=0.54 with varying, Bi and Pb stoichiometries in order to account for the effects of volatility. Ceramic samples were prepared by the standard solid-state reaction method. Starting powders of PbO (99.9 %, Sigma-Aldrich), Bi_2O_3 (99.9 %, Sigma-Aldrich), TiO_2 (99.0 %, Sigma-Aldrich), NiO (99.99 %, Sigma-Aldrich), and Sc_2O_3 (99.995 %, Stanford Materials Corp.) were batched and milled with yttria-stabilized zirconia milling pellets for 6 h in a vibratory milling machine. Batched powders were then dried in an oven at 100 °C, after which dried samples were calcined at 950 °C for 4 h; heating and cooling rates were 3 °C/minute. Calcined powders were milled for another 6 h and dried. Powders were then pressed, ~34.5 MPa, into green discs with polyvinyl butyral (PVB) used as the binder. Discs were then heated to 400 °C at a 5 °C/minute heating rate, and held for 4 h to burn off the binder, after which the discs were heated up to 1150 °C at a 3 °C/minute heating rate and held for fours. Newly sintered ceramic samples were then polished down to a thickness of approximately 0.800 mm to obtain an approximate diameter to thickness ratio of approximately 10:1.

The crystal structure of polished ceramics was determined by x-ray diffraction (Bruker AXS Inc. D8 Discover, Madison, WI, USA). Silver paste was then applied to samples and electrodes were fired at 700 °C for 30 min. Samples were then placed in between two Pt electrodes within an alumina tube (NorECs AS ProbostatTM, Oslo, Norway) and heated up to 650 °C for 1 h. Using a LCR meter (Agilent 4263B, Santa Clara, CA), the dielectric permittivity and loss were measured on un-poled samples, as a function of temperature, measured by a temperature reader (Dpi32-C24, Omega Engineering, Inc., Stamford, CT).

Poling of specimens was conducted inside an environmental chamber (Delta Design Inc., San Diego, CA). Samples were place between two electrodes and heated up to 100 °C for 1 h. A DC electric field of 40 kV/cm was then applied across the samples for 30 min. After 30 min, the ceramics were taken out of the furnace and allowed to cool down to room temperature while the field was still applied for another 30 min. Hysteresis and electromechanical strain measurements were taken inside a standard ferroelectric testing system (Radiant Technologies, Premier Precision II), Albuquerque, New Mexico at room temperature. The field applied was 40 kV/cm and the hysteresis measurement frequency was 1 Hz following similar bulk ferroelectric measurement applications [19, 30]. Strain measurements were averaged over five loops while using a fiber-optic sensor (MTI-2100 Fotonic Sensor, MTI Instruments Inc., Albany, NY). The converse piezoelectric coefficient (d_{33}^* [pm/V]) is calculated from the ratio of the maximum unipolar strain and the maximum applied electric field [10, 31].

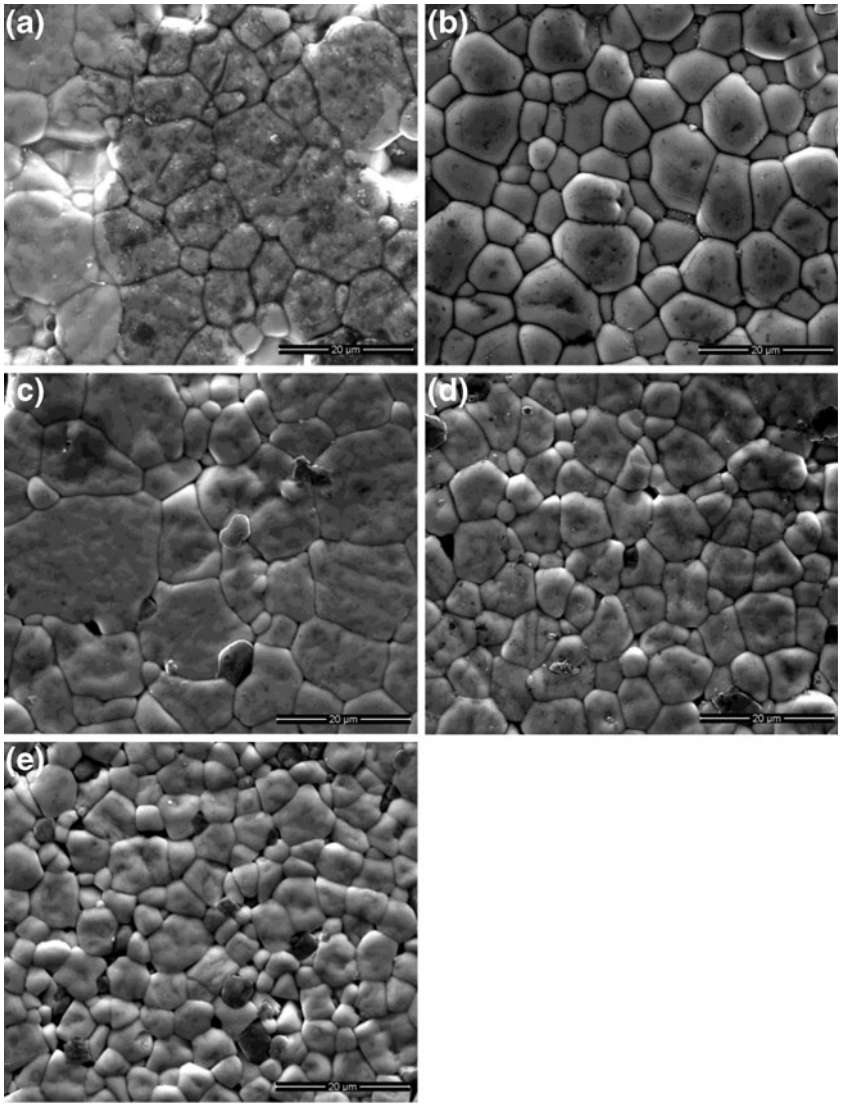

Fig. 1 Electron microscope images of Pb and Bi excess compositions, **a** 5 % Pb excess, **b** 2 % Pb excess, **c** stoichiometric, **d** 2 % Bi excess, and **e** 5 % Bi excess samples

Three different methods were used to measure the depoling temperature T_D: an ex-situ d_{33} technique, analysis of the dielectric loss in log scale, and impedance spectroscopy. For the ex-situ d_{33} approach, poled samples were placed in a furnace and heated to temperatures ranging from 100 °C to 350 °C in 25 °C steps, and held at the measurement temperature for 1 h. After which the samples were cooled down to room temperature and the direct piezoelectric coefficient (d_{33} [pC/N]) was measured using a YE2730A d_{33} meter (Sinoceramics Inc., Shanghai, China). Following the resonance method set by the IEEE standard on piezoelectrics [32], poled samples were placed in the same set-up as the dielectric measurements and heated to incrementally higher temperatures from room temperature up to 400 °C. The samples were allowed to soak at predetermined temperatures for an hour after which an impedance spectrum is measured for frequencies from 1 Hz to 1 MHz.

Measurements of grain size started with the microstructural imaging by the field emission scanning electron microscope (SEM) Quanta ™ 600 FEG SEM (FEI Company, Hillsboro, OR, USA). Afterwards the Abrams Three-Circle procedure, stated in the standard testing methods of the

Table 1 Average grain sizes and % relative accuracy for bismuth and lead excess compositions and the stoichiometric sample [33]

	5 % Pb excess	2 % Pb excess	Stoichiometric	2 % Bi excess	5 % Bi excess
Average Grain Size [µm]	18.0	12.7	20.1	12.6	9.31
% Relative Accuracy	8.1	10.0	8.7	9.5	5.8

American Society for Testing and Materials was applied to SEM images to determine the average grain sizes [33]. According to the ASTM standard, a % relative accuracy of no more than 10 % is acceptable when presenting grain size measurements.

3 Results

3.1 Structural and dielectric properties

In previous work [29], the authors studied the MPB composition of the ternary PT-BS-BNiT system. Compositions were made with 2 % extra Pb added to avoid lead loss. As will be seen later, single-phase compositions were obtained for different amounts of lead or bismuth added or removed. Samples were produced with at least ~94 % theoretical density. The microstructure of the stoichiometric composition as well as the Pb and Bi excess compositions are shown in Fig. 1. The micrographs confirm the high sintered densities with very little porosity. The estimated average grain sizes are listed in Table 1 with the corresponding percent relative accuracy (%RA) referenced in the ASTM standard [33]. Figure 2 shows the diffraction patterns for compositions with varying bismuth and lead stoichiometries for the MPB composition. An increase in the tetragonal splitting of the (00*l*) reflections was observed for compositions deficient in Bi. The perovskite compound $BiScO_3$ was shown to be the rhombehedral analog to $PbZrO_3$ in the PZT system [9, 13]. Therefore, in PT-BS-BNIT, it appears that introducing Bi deficiency near the MPB shifts the overall composition to the tetragonal side of the MPB. This is consistent with the results shown in Fig. 2(b), where an increase in the tetragonal splitting was observed for an increase in Pb content.

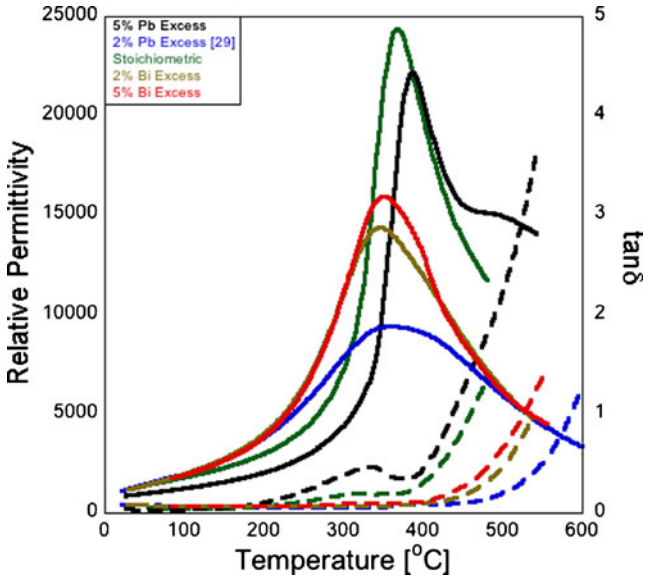

Fig. 3 Dielectric permittivity and loss lead and bismuth excess MPB compositions with a frequency of 10 kHz. The dielectric loss was plotted with dotted lines while the permittivity was plotted down with the solid lines

In order to determine the Curie temperature of the samples, dielectric measurements were carried out on un-poled samples. The results at 10 kHz are plotted in Fig. 3, with the stoichiometric composition compared to compositions with 2 % and 5 % excess Pb and Bi. Both bismuth excess samples and the 2 % Pb excess sample were shown to have a

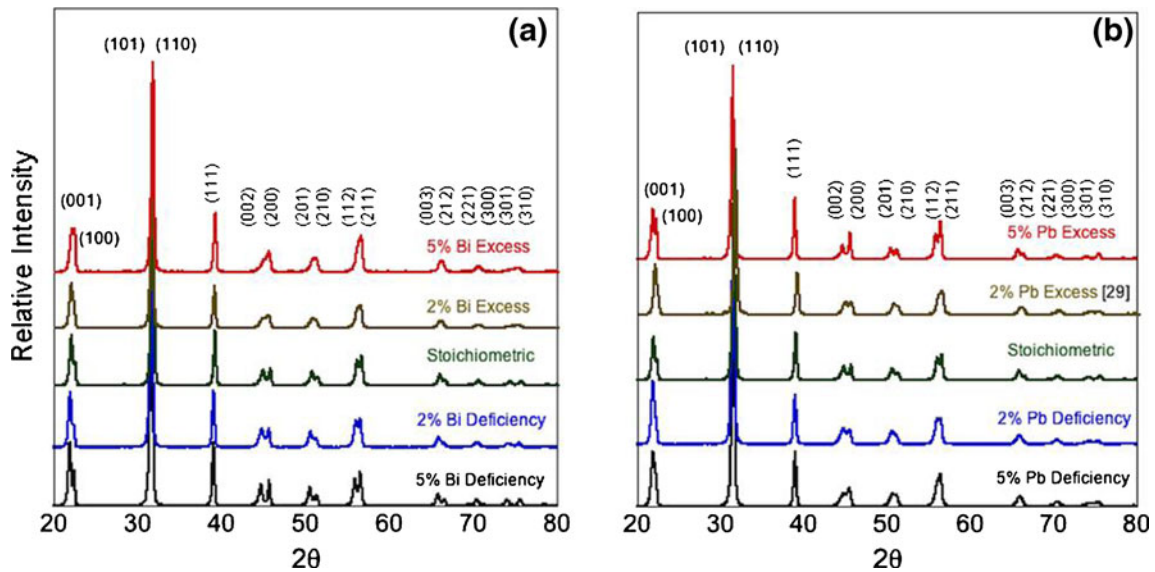

Fig. 2 X-ray diffraction of samples of MPB composition with varying stoichiometries: **a** Bi-deficient or Bi-excess samples compared to XRD scan of the stoichiometric composition and **b** likewise for changes to Pb content compared to stoichiometric MPB composition

Table 2 Dielectric properties of the MPB ($xPbTiO_3$-(1-x)[$BiScO_3$ + $Bi(Ni_{1/2}Ti_{1/2})O_3$] ternary at room temperature and 100 °C

Stoichiometry	25 °C		100 °C	
	Dielectric constant ε_r	Dielectric loss $tan\delta$	Dielectric constant ε_r	Dielectric loss $tan\delta$
5 % Pb-excess	920	0.033	1310	0.061
2 % Pb-excess [29]	1290	0.070	2150	0.062
2 % Pb-deficient	1330	0.067	2100	0.061
5 % Pb-deficient	1410	0.046	2590	0.071
Stoichiometric	1490	0.049	1915	0.053
5 % Bi-excess	1320	0.067	2070	0.064
2 % Bi-excess	1310	0.068	2170	0.062
2 % Bi-deficient	1345	0.062	2000	0.052
5 % Bi-deficient	1250	0.035	1700	0.038

relatively low T_C of approximately 350 °C. There were some noted differences in the diffuseness of the phase transition, with the 2 % Pb excess composition being the most diffuse. The 5 % Pb excess and the stoichiometric samples had transition temperatures of 390 °C and 370 °C, respectively. The dielectric loss remained below the 0.1 % threshold up until 220 °C except for the 5 % Pb excess sample in which the loss increased above 0.1 % around 200 °C. Table 2 lists the dielectric properties measured at 1 kHz at temperatures of 25 °C and 100 °C.

3.2 Ferroelectric and piezoelectric properties

The ferroelectric hysteresis properties were measured on poled samples and plotted in Fig. 4. Samples with varying Bi stoichiometry, shown in Fig. 4(a), show a coercive field between 24 and 25 kV/cm for all samples except 5 % Bi-deficient sample, which had a coercive field of 28 kV/cm. All hysteresis loops show saturation at an applied field of 40 kV/cm except for the 5 % Bi-deficient sample, which showed decreased saturation polarization and remanent polarization compared to the stoichiometric sample. With an increased amount of bismuth, the remanent polarization increased to values of 36.5 μC/cm^2 and 40.5 μC/cm^2 for the 2 % and 5 % Bi-excess compositions, respectively. The remanent polarization of the 2 % Bi-deficient sample was 33.0 μC/cm^2 while the 5 % Bi-deficient had a remanent polarization of 27.9 μC/cm^2. Both bismuth excess compositions and the 2 % Bi-deficient sample had a higher remanent polarization than the stoichiometric composition of P_r=31.0 μC/cm^2. As shown in Fig. 4(b), all of the lead excess compositions showed significantly lower remanent polarizations than the bismuth excess compositions. The remanent polarizations of the 5 % and 2 % Pb-excess

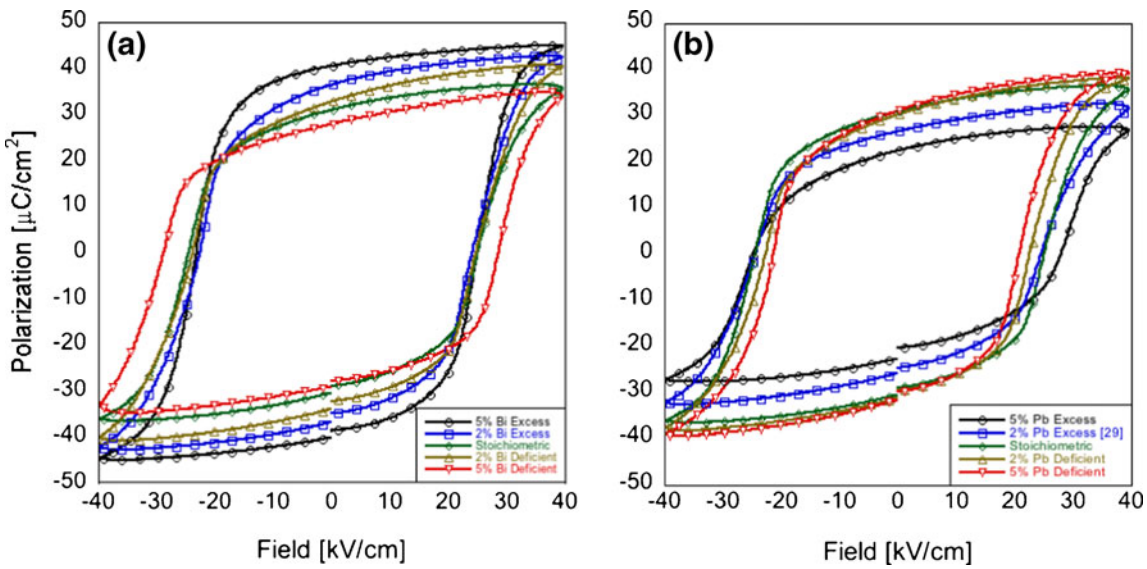

Fig. 4 Polarization hysteresis of Bi (**a**) and Pb (**b**) deficient and excess samples compared to the stoichiometric composition

samples were 22.5 μC/cm^2 and 26.4 μC/cm^2 [29] respectively. For the lead deficient compositions, the remanent polarizations were P_r=31.0 μC/cm^2 and P_r=30.2 μC/cm^2 for 5 % and 2 % Pb-deficient samples, respectively. The coercive field for the lead excess and deficient samples exhibited a wider range of values from 21 to 28 kV/cm as compared to the bismuth compositions.

Figure 5 shows both bipolar and unipolar electromechanical strain measurements on bismuth and lead samples poled at 40 kV/cm at 100 °C for 30 min. In Fig. 5(a), the bipolar strain behavior of bismuth deficient and excess compositions showed the characteristic asymmetric "butterfly" loops due to degradation of poled domains as result of field switching. The bismuth excess compositions showed the highest amount of strain at approximately 0.35 %. Bismuth deficient samples exhibited similar strain values to the stoichiometric composition between 0.2 % and 0.3 %. In Fig. 5(c), lead excess and deficient samples showed strains of about 0.25 % for the 2 % Pb-deficient and 5 % Pb-excess samples while

Table 3 Room temperature piezoelectric coefficient measured from d_{33} meter (direct) and calculated from unipolar strain (converse)

Stoichiometry	d_{33} [pC/N]	d_{33}^* [pm/V]
5 % Pb-excess	171	549
2 % Pb-excess [29]	376	547
2 % Pb-deficient	370	688
5 % Pb-deficient	380	473
Stoichiometric	340	896
5 % Bi-excess	413	492
2 % Bi-excess	445	701
2 % Bi-deficient	425	695
5 % Bi-deficient	343	682

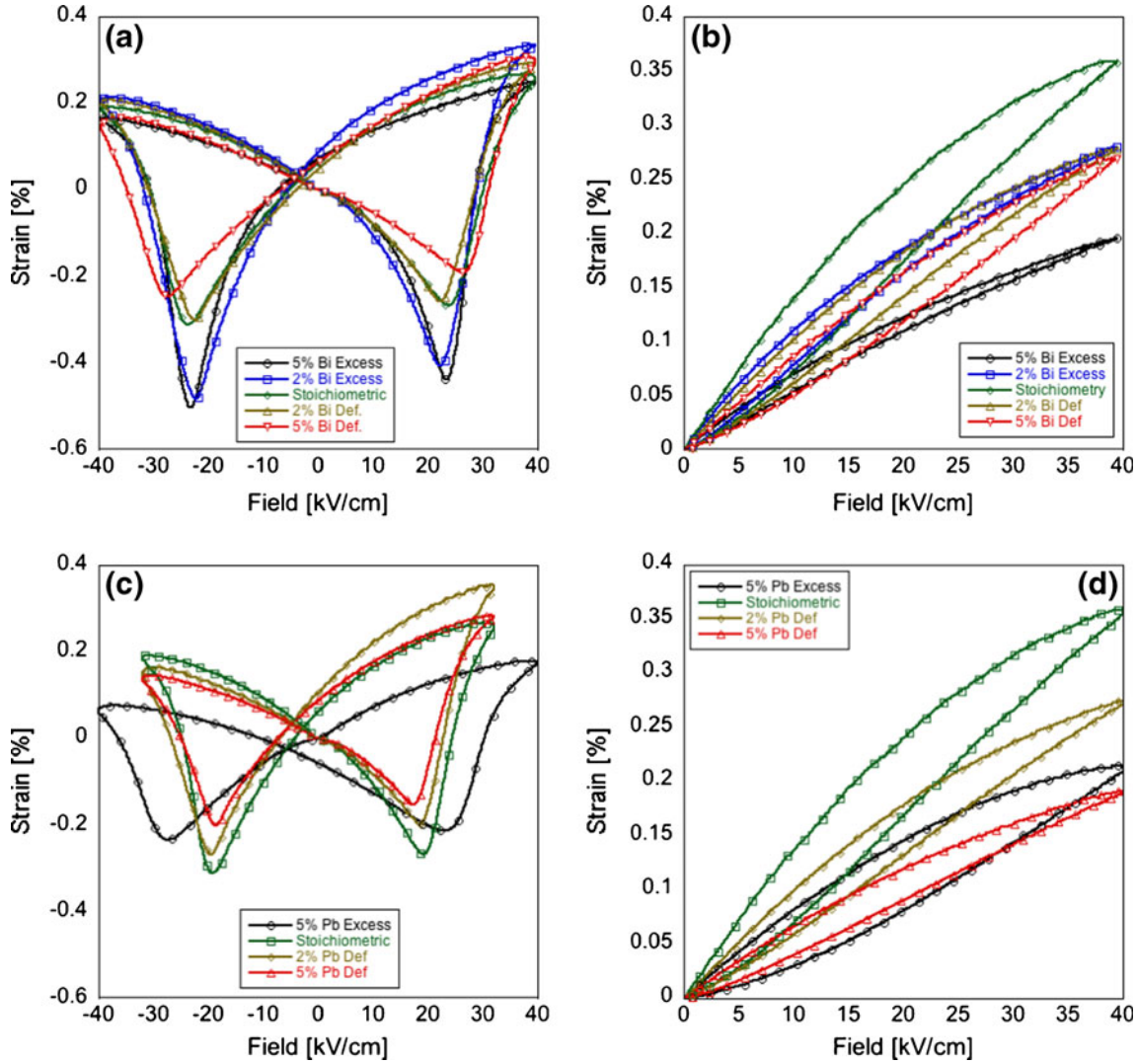

Fig. 5 Electromechanical strain, both bipolar (**a**) and unipolar (**b**), of stoichiometric, 2 %, and 5 % bismuth, lead excess and deficient samples. A 2 % Pb-excess sample was created in a previous work, which the reader is directed [29]

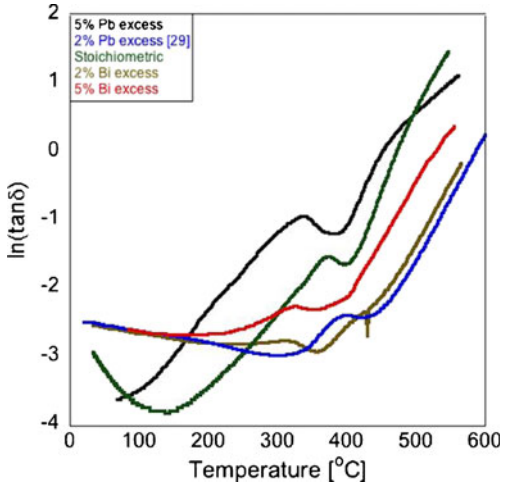

Fig. 6 Dielectric dissipation plotted again in log scale for lead and bismuth excess samples compared to the stoichiometric composition; measurements taken at 10 kHz

the 5 % Pb-deficient sample exhibited strain values close to 0.2 %. In Fig. 5(b) and (d), unipolar strain measurements are presented for bismuth and lead respectively in order to calculate the high field d_{33}^* constants. The d_{33}* values of the stoichiometric composition was approximately 900 pm/V and compositions with variations in bismuth and lead stoichiometry varied between 470 and 700 pm/V. The results for all compositions are compiled in Table 3.

3.3 Depoling temperature

From measurement of the dielectric constant versus temperature (Fig. 3), the Curie temperature was observed to be between 350 °C and 390 °C depending on the composition. However, a local maximum in the dielectric loss was observed at temperatures 10 to 20 °C below T_C for all samples. Plotting the value for tan δ in a log scale as shown in Fig. 6, the dielectric anomaly corresponding can be more easily determined. Using the approach outlined by Leist et al. [12], the depolarization temperature (T_D) for the stoichiometric composition was approximately 320 °C compared to the maximum measured at 400 °C for the 2 % Pb excess composition [29]. As the bismuth content increased the depolarization temperature dropped to 324 °C and 305 °C for the 2 % and 5 % Bi excess samples, respectively. To confirm the depolarization temperature obtained from the dielectric data, two other methods were utilized: an ex-situ d_{33} measurement and analysis of the piezoelectric coupling coefficient from high temperature impedance spectra.

The ex-situ d_{33} data is presented in Fig. 7. The depolarization temperatures are determined from the temperature at which the piezoelectric coefficient experienced a significant decrease; below this temperature, the piezoelectric constant should remain independent of temperature. The highest piezoelectric coefficient observed was 445 pC/N for the 2 % Bi excess sample, which remained constant up to a temperature of approximately 275 °C. At approximately 300 °C, the piezoelectric constant decreased to zero, therefore $T_D \approx 300$ °C for the 2 % Bi-excess composition. For the stoichiometric composition, the piezoelectric coefficient saw an initial decrease to 250 pC/N and remained constant up to 325 °C. The depolarization temperature measured from this ex-situ approach and the dielectric data were very similar for the stoichiometric sample: 320 °C and 325 °C, respectively. In Fig. 7(b), both Pb-excess and Pb-deficient samples maintained low piezoelectric coefficients between 150 pC/N and 250 pC/N depending on composition up to temperatures

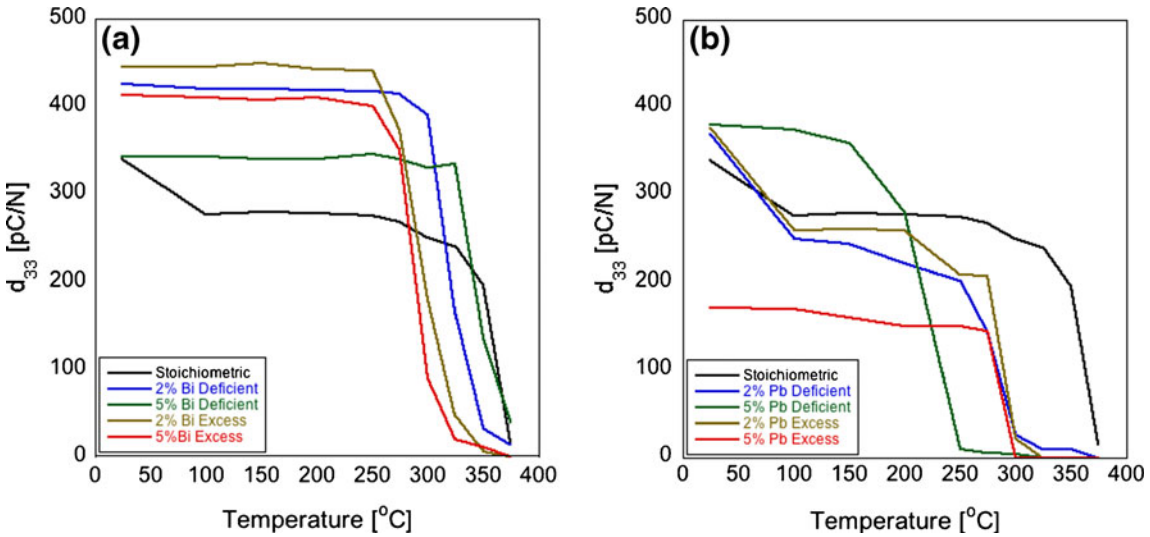

Fig. 7 Ex-situ d_{33} plots of the various stoichiometries of the MPB composition, **a** Bi-excess and Bi-deficient on the left hand side and **b** Pb-excess and Pb-deficient on the right hand side

Table 4 Depolarization temperatures (°C) measured through dielectric data, ex-situ d_{33}, and high temperature impedance

Stoichiometry	Dielectric loss (10 kHz) in log scale	Ex-situ d_{33}	High temperature impedance
5 % Pb-excess	334	275	300
2 % Pb-excess	400	275	–
2 % Pb-deficient	345	275	–
5 % Pb-deficient	325	200	225
Stoichiometric	320	325	325
5 % Bi-excess	305	300	–
2 % Bi-excess	324	300	300
2 % Bi-deficient	340	325	310
5 % Bi-deficient	345	325	–

of approximately 300 °C. One notable exception was the 5 % Pb-deficient composition, which had a piezoelectric coefficient of 375 pC/N and a depolarization temperature of only 250 °C.

Another method for determining the depolarization temperature involved measuring the impedance spectra as a function of temperature and then, by following the IEEE standard [32], calculating the planar mechanical coupling factor, k_p,. For the stoichiometric composition, 2 % Bi excess and deficient, and 5 % Pb excess and deficient samples, the impedance was measured up to 400 °C. Here, as with the ex-situ d_{33} method, the depolarization temperature was determined from the temperature at which a decrease in the value of k_p was observed. Most of the compositions exhibited a decrease in k_p at temperatures between 300 °C and 325 °C. The only exception was the 5 % Pb-deficient composition, which observed a decrease in k_p at 225 °C. The results of all three methods of determining the depolarization temperature for different Pb and Bi stoichiometry are summarized in Table 4.

4 Discussion

As seen in Table 3, samples with excess bismuth exhibited higher low-field piezoelectric constants, however, the stoichiometric composition exhibited the highest d_{33}^* value. Dielectric loss and permittivities listed in Table 2 for both Pb and Bi excess samples were similar, however, the 5 % Pb excess and stoichiometric compositions had lower dielectric loss at both room temperature and at 100 °C. The average grain sizes for the stoichiometric, and all the lead and bismuth excess compositions fell into the range of 10–21 μm. The stoichiometric composition had the largest grain size with an average grain size of 20.1 μm. Possibly due to the larger grain size in the stoichiometric composition, the dielectric and piezoelectric properties were improved to the properties of the compositions with excess oxides.

As grain sizes increased, the number of grains decreased and thus the volume of grain boundaries also decreased leading to an increase in resistivity. Research conducted on liquid phase-sintered PT-BS by Sehirlioglu et al. [34] showed an increase in resistivity led to an improvement in poling conditions and in turn, an improvement in piezoelectric properties. Sehirlioglu also found that increasing the amount of PbO in PT-BS increased the grain-boundary conductivity leading to a decrease in piezoelectric properties while adding Bi_2O_3 improved the resistivity and piezoelectric properties of PT-BS. Liquid phase sintering was not specifically part of the present study, however, the larger grain sizes that resulted from the stoichiometric composition led to higher dielectric and high field piezoelectric constants and lower dielectric losses. The replacement of lead by bismuth on the A-site and/or the creation of lead vacancies alone may be responsible for the improved resistivity and the improved low field piezoelectric coefficients for the Bi excess samples [34]. The Pb excess compositions exhibited an increased tetragonality, which led to an increase in T_C and T_D [24].

5 Conclusion

The MPB composition of the ternary perovskite PT-BS-BNiT was studied extensively to determine the transition temperature and depolarization temperature. Other important ferroelectric properties were also characterized including: both low and high field d_{33} and d_{33}^* constants, dielectric permittivity and loss, polarization hysteresis, and electromechanical strain. The stoichiometry of the MPB composition was adjusted by changing the A-site occupancy of Bi and Pb to optimize the depoling temperature and the ferroelectric properties. It was found that the addition of 2 % Bi led to improved low field piezoelectric properties with the Curie temperature, T_C=346 °C, and more importantly the depolarization temperature, T_D=300 °C, remained relatively high. Room temperature permittivity of the 2 % Bi-excess sample was 1320 at 1 kHz with a loss of 0.067. The highest low field piezoelectric coefficient was observed for the 2 % Bi-excess sample with d_{33}=445 pC/N while the stoichiometric composition had the highest high field

coefficient with d_{33}^*=896 pm/V. The remanent polarization of the stoichiometric and the 2 % Bi-excess compositions were 31.0 μC/cm^2 and 36.4 μC/cm^2, respectively, while the maximum remanent polarization was observed for the 5 % Bi-excess sample with P_r=41.0 μC/cm^2. Bipolar electromechanical strain applied to the 2 % Bi-excess sample caused strains up to 0.5 % compared to strains of 0.25 % of the stoichiometric composition under an applied field.

Acknowledgement The authors would like to acknowledge this work was supported in part through NASA/Oregon Space Grant Consortium, grant NNX10AK68.

References

1. J. Valasek, Phys Rev **17**, 475–481 (1921)
2. K. Yamakawa, K. Imai, O. Arisumi, T. Arikado, M. Yoshioka, T. Owada, K. Okumura, Jpn. J. Appl. Phys. **41**, 2630–2634 (2002)
3. L.F. Malmonge, J.A. Malgonge, W.K. Sakamoto, Mater Res **6**, 469–473 (2003)
4. N. Makki, R. Pop-Iliev, Microsyst Technol **18**, 1201–1212 (2012)
5. S. Matsushita, I. Kanno, K. Adachi, R. Yokokawa, H. Kotera, Microsyst Technol **18**, 765–771 (2012)
6. R.C. Turner, P.A. Fuierer, R.E. Newnham, T.R. Shrout, Appl Acoust **41**, 299 (1994)
7. T.R. Shrout, S.J. Zhang, J. Electroceram. **19**, 111–124 (2007)
8. Y. Jiang, Y. Jiang, W. Shi, L. Li, Q. Chen, X. Yue, D. Xiao, J. Zhu, Ferroelectrics **380**, 130–134 (2009)
9. B. Jaffe, W.R. Cook, H. Jaffe, *Piezoelectric Ceramics* (Academic, New York, 1971)
10. G.H. Haertling, J. Am, Ceram. Soc. **82**, 797–818 (1999)
11. A. Sehirlioglu, A. Sayir, F. Dynys, J. Am, Ceram. Soc. **93**, 1718–1724 (2010)
12. T. Leist, J. Chen, W. Jo, E. Aulbach, J. Suffner, J. Rödel, J. Am, Ceram. Soc. **95**, 711–715 (2012)
13. R.E. Eitel, C.A. Randall, T.R. Shrout, P.W. Rehrig, W. Hackenberger, S.-E. Park, Jpn. J. Appl. Phys. **40**, 5999–6002 (2001)
14. R.E. Eitel, S.J. Zhang, T.R. Shrout, C.A. Randall, J. Appl, Phys. **96**, 2828–2831 (2004)
15. R.E. Eitel, C.A. Randall, T.R. Shrout, S.-E. Park, Jpn. J. Appl. Phys. **41**, 2099–2104 (2002)
16. C.J. Stringer, T.R. Shrout, C.A. Randall, I.M. Reaney, J Appl Phys **99**, 0241061 (2006)
17. S.J. Zhang, C.A. Randall, T.R. Shrout, Appl Phys Lett **83**, 3150–3152 (2003)
18. A. Sehirlioglu, A. Sayir, F. Dynys, J. Appl, Phys. **106**, 0141021–0141027 (2009)
19. Y. Shimojo, R. Wang, T. Sekiya, T. Nakamura, L.E. Cross, Ferroelectrics **284**, 121–128 (2003)
20. C.A. Randall, R.E. Eitel, T.R. Shrout, D.I. Woodward, I.M. Reaney, J. Appl, Phys. **93**, 9271–9274 (2003)
21. T. Takenaka, M. Yamada, Jpn. J. Appl. Phys. **32**, 4218–4222 (1993)
22. S.M. Choi, C.J. Stringer, T.R. Shrout, C.A. Randall, J. Appl, Phys. **98**, 0341081–0341084 (2005)
23. J. Chen, X. Sun, J. Deng, Y. Liu, J. Li, X. Xing, J Appl Phys **105**, 044105 (2009)
24. M.R. Suchomel, P.K. Davies, Appl Phys Lett **86**, 2629051–2629053 (2005)
25. S. Sharma, D.A. Hall, J. Mater, Sci.: Mater. Electron. **21**, 405–409 (2010)
26. T. Sebastian, I. Sterianou, D.C. Sinclair, A.J. Bell, D.A. Hall, I.M. Reaney, J. Electroceram. **25**, 130–134 (2010)
27. I. Sterianou, I.M. Reaney, D.C. Sinclair, D.I. Woodward, D.A. Hall, A.J. Bell, T.P. Comyn, Appl Phys Lett **87**, 242901 (2005)
28. I. Sterianou, D.C. Sinclair, I.M. Reaney, T.P. Comyn, A.J. Bell, J Appl Phys **106** (2009)
29. T.Y. Ansell, D.P. Cann, Mater Lett **80**, 87–90 (2012)
30. Y. Inaguma, A. Miyaguchi, M. Yoshida, T. Katsumata, Y. Shimojo, R. Wang, T. Sekiya, J. Appl, Phys. **95**, 231–235 (2004)
31. R.E. Eitel, T.R. Shrout, C.A. Randall, J Appl Phys **99**, 124110 (2006)
32. ANSI/IEEE 176-1987, IEEE Standard on Piezoelectricity, IEEE, New York, 1987
33. Standard Test Methods for Determining Average Grain Size, American Society for Testing and Materials, ASTM International, 100 Barr Harbor Drive, PO Box C700, West Conshohocken, PA 19428-2959. United States, 2010
34. A. Sehirlioglu, A. Sayir, F. Dynys, J. Am, Ceram. Soc. **91**, 2910–2916 (2008)